Nuclear Instruments and Methods in Physics Research B 106 (1995) 438-441

ELSEVIER

NIM B
Beam Interactions with Materials & Atoms

Photorefractive waveguides produced by ion-implantation of fused silica

M. Verhaegen [a], L.B. Allard [a], J.L. Brebner [a,*], M. Essid [a], S. Roorda [a], J. Albert [b]

[a] *Groupe de recherche en physique et technologie des couches minces, Physics Department, Université de Montréal, P.O. Box 6128, Station "Centre-ville", Montréal, Québec H3C 3J7, Canada*

[b] *Communications Research Centre, P.O. Box 11490, Station H, Ottawa, Ontario K2H 8S2, Canada*

Abstract

The implantation of 5 MeV silicon and germanium ions into silica forms a 4 μm thick optical waveguide near the substrate's surface with a refractive index change related to that of the delivered damage. These waveguides are photosensitive due to the presence of color centres created during implantation which can be bleached by laser light illumination. We measure the optical absorption, the compaction and the refractive index of implanted samples as a function of dose. We compare the absorption bleaching efficiency of ArF and KrF excimer laser light on two similar samples and observe an overall efficiency two orders of magnitude higher in the ArF case.

1. Introduction

For almost twenty years it has been known that the refractive index of doped silica optical fibres can be modified permanently by exposure to UV-light [1]. Photosensitivity is now extensively used to fabricate optical devices such as Bragg gratings [2,3] and channel waveguides [2,3]. Despite this progress in terms of applications, a thorough understanding of the physical phenomena responsible for the photosensitivity is still lacking.

It was recently observed that photosensitivity can be induced in synthetic fused silica by implantation of germanium ions [4]. This procedure leads to the formation of strong absorption bands which can be bleached with 248 nm KrF excimer laser light. In addition to the formation of strong absorption bands near 163, 212 and 243 nm, the ion-implantation (of Si as well as Ge) increases the refractive index of silica in a 3 to 5 μm thick layer near the implanted surface, thus forming an optical waveguide. We have bleached these absorption bands using ArF (193 nm) and KrF (248 nm) excimer laser pulses in order to compare the bleaching efficiency at these two wavelengths.

2. Experimental

0.5 mm thick high-purity synthetic fused silica substrates (Suprasil-2, Heraeus Amersil Inc.) were implanted at room temperature in a vacuum of 10^{-7} Torr with 5 MeV Si^{2+} or Ge^{3+} ions using the Université de Montréal 6 MV Tandem accelerator. In the case of the Si-implantation, the ion beam had a diameter of 3 mm, its current was 500 nA, it was scanned over an area of 4 cm^2 on the sample and the implanted doses ranged from 3×10^{13} to 3×10^{17} ions/cm^2. For the Ge-implantation the parameters were the same except for the current which was typically 150 nA.

The optical absorption measurements in the 190 to 400 nm wavelength range were carried out using a Cary-5 spectrophotometer. The bleaching of the absorption bands was performed by 20 ns excimer laser pulses from a Lumonics excimer laser model 500 operating with either ArF (193 nm, 6.4 eV) or KrF (248 nm, 5.0 eV) gas mixtures. Thickness changes induced by implantation were measured with a DEKTAK 3030 ST profilometer and the variation of refractive index measurements were performed using an Abbe refractometer at 589 nm by taking the difference of implanted and virgin silica index values.

3. Results and discussion

Silicon and germanium ions were implanted to doses ranging between 3×10^{13} and 3×10^{17} ions/cm^2. Ions impinging on a substrate initially cause it to undergo compaction in the implanted region. As seen in Fig. 1, the step height at the frontier between implanted and virgin regions increases with dose up to a dose of 10^{16}

* Corresponding author. Tel. +1(514)343-6614, fax +1(514)343-2071, e-mail brebnerj@ere.umontreal.ca.

0168-583X/95/$09.50
SSDI 0168-583X(95)00748-2

Si/cm^2. Beyond this dose, the step height is observed to decrease. It is possible that this behavior is due to the increasingly significant effect of the amount of material added to the implanted region and which is not taken into account in Fig. 1. On the same figure is shown the behavior of the refractive index variation as a function of dose. The increase in this variation is mainly attributable to a densification of the material and, to a lesser extend, to the creation of color centres. The nature of the apparent decrease at higher doses is not clearly understood.

From absorbance measurements we obtain the absorption coefficient as a function of photon energy for different Si doses as shown in Fig. 2. At doses of 10^{15} Si/cm^2 and lower, the intensities of the B_2 (5.01 eV), E′ (5.85 eV) and E (7.6 eV) bands increase monotonically. We see only the low energy tail of the E band which has been identified from absorption measurements in the vacuum UV. These spectra reveal a strong band at 7.6 eV in similarly implanted samples. At these low doses, Gaussian lineshapes were adequate for fitting the data. For doses of 10^{16} Si/cm^2 and beyond, the absorption coefficients strongly increase and the absorption bands can no longer be fitted by Gaussian lineshapes alone. A background absorption coefficient having an ω^4 dependence must be added to obtain an adequate fit, where ω is the angular frequency of the photons. This indicates the presence of Rayleigh scattering, i.e. scattering from Si clusters whose presence was separately confirmed by TEM measurements which showed cluster ~ 8 nm in diameter.

Fig. 3 compares the effects of ArF and KrF excimer laser light illumination on similarly ion-damaged samples. As observed, the initial absorption coefficient spectra in both the 10^{15} Si/cm^2 and the 10^{14} Ge/cm^2 samples are similar and thus comparable since the

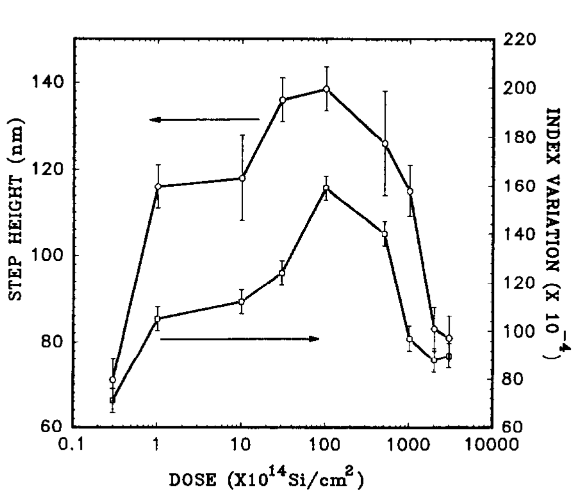

Fig. 1. Step height and refractive index variation data for 5 MeV Si^{2+} -implanted silica as a function of implanted dose.

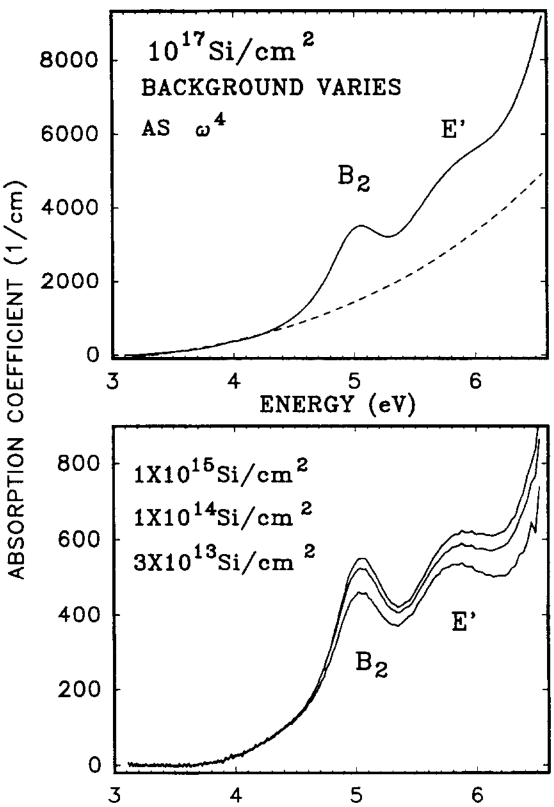

Fig. 2. The bottom graph shows the absorption coefficient as function of photon energy for Si-implanted samples. The order in which the traces appear corresponds to the order of the indicated doses. The top graph shows the absorption coefficient for samples implanted to a dose of 10^{17} Si/cm^2. The dashed line appearing is indicative of the ω^4 background attributable to Rayleigh scattering.

presence of the absorption bands is related to delivered damage rather than to the ion species. The most striking feature is the difference in the amount of integrated delivered energy required to bleach the absorption spectra. For instance only 1.26 J/cm^2 of 6.4 eV photons (ArF, top graph) is required to bleach the absorption to the same level attained when bleaching with 55 J/cm^2 of 5.0 eV photons (KrF, bottom graph). Though the ArF bleaching efficiency is much higher, measurements carried out with higher energy resolution with KrF bleaching show what appears to be a resonant bleaching effect between the B_2 band and the KrF laser line, both of which lie at the same energy. In fact the B_2 band is observed to significantly decrease with single KrF laser pulses while the remainder of the absorption spectrum remains unchanged. The B_2 band disappears after having been irradiated with 300 mJ/cm^2 only. By applying Smakula's equation [5,6], which relates the area of a given absorption band to the number of color centres giving rise to it, we obtain

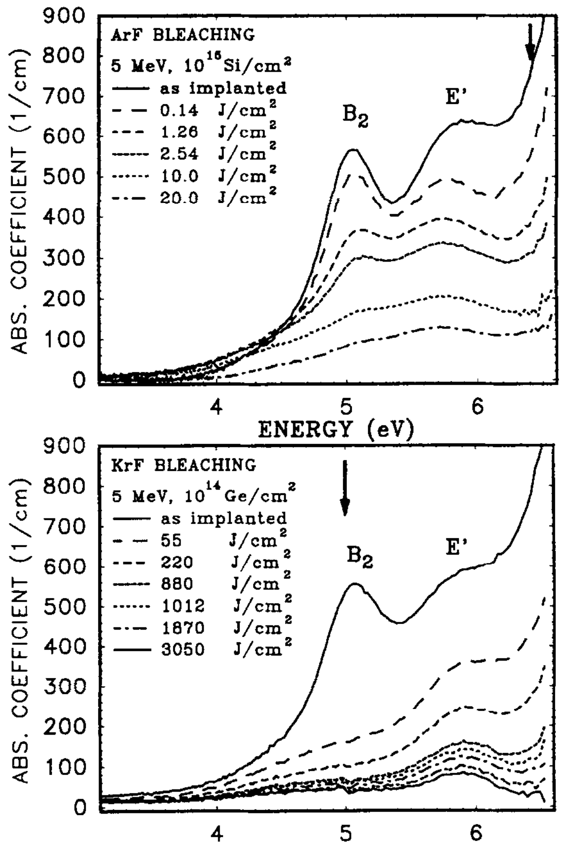

Fig. 3. The top graph shows the absorption spectra at different stages of ArF excimer laser light bleaching of high-purity synthetic fused silica implanted to a dose of 10^{15} Si/cm^2. The bottom graph shows the absorption spectra at different stages of KrF excimer laser light bleaching of the same type of silica implanted to a dose of 10^{14} Ge/cm^2. The energies appearing in the legends are the cumulative energies delivered to the samples. The arrows indicate the laser line energies.

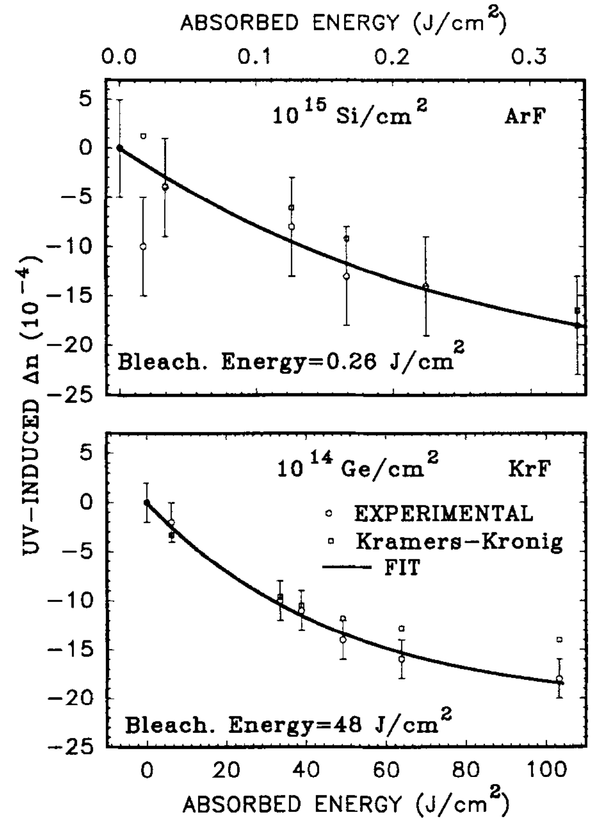

Fig. 4. UV-induced refractive index variation as a function of absorbed ArF (top) and KrF (bottom) energy. The circles are the data obtained with an Abbe refractometer, the squares are the data obtained by a Kramers–Kronig treatment of the absorption data of Fig. 3 and the solid lines are the fitted decaying exponentials. The bleaching energies obtained through these fits are 0.26 J/cm^2 for the ArF case and 48 J/cm^2 for the KrF case.

the 1/e bleaching energies of the absorption bands. In the case of ArF bleaching, these are 0.21 J/cm^2 for the E band, 0.21 J/cm^2 for the E′ band and 0.16 J/cm^2 for the B_2 band. In the case of KrF bleaching, the bleaching energies are 17.4 J/cm^2 for the E band, 6.12 J/cm^2 for the E' band and 1.87 J/cm^2 for the B_2 band (preliminary higher energy resolution bleaching measurements not shown on Fig. 3. yield a bleaching energy of 12 mJ/cm^2 which clearly indicates a resonance phenomenon).

The UV-induced refractive index changes are shown on Fig. 4. The results obtained through a Kramers–Kronig analysis of the absorption spectra shown on Fig. 3 are consistent with those obtained by direct index measurements obtained with an Abbe refractometer. In both ArF and KrF cases, the total index change is 0.0018 and decaying exponentials fitted to these data yield bleaching energies consistent with those obtained for the separate bands via Smakula's equation, viz. the bleaching energy of KrF is two orders of magnitude larger than for ArF.

4. Conclusion

In our study of the effect of ion-implantation-induced photosensitivity in high-purity synthetic fused silica we have observed the following. Firstly a step height increase with implanted dose was observed up to a dose of 10^{16} Si/cm^2 followed by a decrease as the dose reached 3×10^{17} Si/cm^2. Refractive index measurements revealed the presence of Si clusters at doses of 10^{16} Si/cm^2 and beyond.

Bleaching of the implantation-created absorption bands was carried out using ArF and KrF excimer laser lines and the efficiency of the ArF bleaching, measured through UV-induced refractive index variation, was two orders of magnitude superior to that of KrF. The bleaching efficiency measured by applying Smakula's equation to the various bands at different stages of the bleaching process also reveals the higher efficiency of ArF over KrF bleaching except in the case of the B_2 band where the efficiency of KrF here surpasses that of all others. The energy position of this band coincides with that of the KrF laser line, thus indicating a resonance phenomenon whose origin remains to be determined.

References

[1] K.O. Hill, Y. Fuji, D.C. Johnson and B.S. Kawasaki, Appl. Phys. Lett. 32 (1978) 647.

[2] V. Mizrahi, P.J. Lemaire, T. Erdogan, W.A. Reed, D.J. DiGiovanni and R.M. Atkins, Appl. Phys. Lett. 63 (1993) 1727.

[3] B. Malo, F. Bilodeau, J. Albert, D.C. Johnson, K.O. Hill, Y. Hibino and M. Abe, SPIE Proc. 2044 (1993) 42.

[4] J. Albert, K.O. Hill, B. Malo, D.C. Johnson, J.L. Brebner, Y.B. Trudeau and G. Kajrys, Appl. Phys. Lett. 60 (2) (1992) 148.

[5] A. Smakula, Physik 59 (1930) 603.

[6] D.Y. Smith and D.L. Dexter, Progress in Optics vol. X, Ed. Emil Wolf (North-Holland, Amsterdam, 1972) Chapter V.